



Synthesis and biological activity of a CXCR4-targeting bis(cyclam) lipid

DOI:

[10.1039/C8OB01439F](https://doi.org/10.1039/C8OB01439F)

Document Version

Accepted author manuscript

[Link to publication record in Manchester Research Explorer](#)

Citation for published version (APA):

Peters, A., McCallion, C., Booth, A., Adams, J. A., Rees-Unwin, K., Pluen, A., ... Webb, S. (2018). Synthesis and biological activity of a CXCR4-targeting bis(cyclam) lipid. *Organic and Biomolecular Chemistry*. <https://doi.org/10.1039/C8OB01439F>

Published in:

Organic and Biomolecular Chemistry

Citing this paper

Please note that where the full-text provided on Manchester Research Explorer is the Author Accepted Manuscript or Proof version this may differ from the final Published version. If citing, it is advised that you check and use the publisher's definitive version.

General rights

Copyright and moral rights for the publications made accessible in the Research Explorer are retained by the authors and/or other copyright owners and it is a condition of accessing publications that users recognise and abide by the legal requirements associated with these rights.

Takedown policy

If you believe that this document breaches copyright please refer to the University of Manchester's Takedown Procedures [<http://man.ac.uk/04Y6Bo>] or contact uml.scholarlycommunications@manchester.ac.uk providing relevant details, so we can investigate your claim.



Synthesis and biological activity of a CXCR4-targeting bis(cyclam) lipid

Received 00th January 20xx,
Accepted 00th January 20xx

DOI: 10.1039/x0xx00000x

www.rsc.org/

Anna D. Peters,^{a,b,†} Catriona McCallion,^{a,b,c,†} Andrew Booth,^{a,b} Julie A. Adams,^c Karen Rees-Unwin,^d Alain Pluen,^e John Burthem,^{c,d,*} Simon J. Webb^{a,b,*}

A bis(cyclam)-capped cholesterol lipid designed to bind C-X-C chemokine receptor type 4 (CXCR4) was synthesised in good overall yield from 2-methoxyphenol through a seven step synthetic route, which also provided a bis(cyclam) intermediate bearing an octaethyleneglycol-primary amine that can be easily derivatised. This bis(cyclam)-capped cholesterol lipid was water soluble and self-assembled into micellar and non-micellar aggregates in water at concentrations above 8 μM . The bioactivity of the bis(cyclam)-capped cholesterol lipid was assessed using primary chronic lymphocytic leukaemia (CLL) cells, first with a competition binding assay then with a chemotaxis assay along a C-X-C motif chemokine ligand 12 (CXCL12) concentration gradient. At 20 μM , the bis(cyclam)-capped cholesterol lipid was as effective as the commercial drug AMD3100 for preventing the migration of CLL cells, despite a lower affinity for CXCR4 than AMD3100.

Introduction

The mammalian C-X-C chemokine receptor type 4 (CXCR4) is a key cell-surface protein that can have a major role in cancer and other illnesses. CXCR4 is targeted by bis(cyclam) containing drugs, which disrupt interactions between the receptor and its conjugate ligand, C-X-C motif chemokine ligand 12 (CXCL12).¹ The bis(cyclam) compound class came to particular prominence in the 1990s due to the central role of CXCR4 in HIV infection, as certain forms of the virus were found to bind and enter T-cells through the receptors CXCR4 and CCR5.¹ The current leader in the bis(cyclam) class of drugs, AMD3100 (plerixafor, Figure 1), is used in the clinic in the context of haematopoietic stem cell transplants. This usage exploits the role of CXCR4 in the retention of stem cells in the bone marrow (BM): AMD3100 disrupts the CXCR4-CXCL12 axis, mobilising the stem cells from the BM and into the vasculature, where the cells can be collected and used for transplant.^{1,2}

Research into the use of AMD3100 to treat chronic lymphocytic leukaemia (CLL) has found that it can disrupt CLL

lymphocyte interactions with cells in the microenvironment, potentially blocking interactions that promote chemoprotection and proliferation of the CLL cells.^{3,4,5} Furthermore, when used in conjunction with standard therapies for other cancers it increased cancer cell death^{6,7,8,9} and forced breast cancer cells out of the bone marrow and into the vasculature *in vivo*.¹⁰

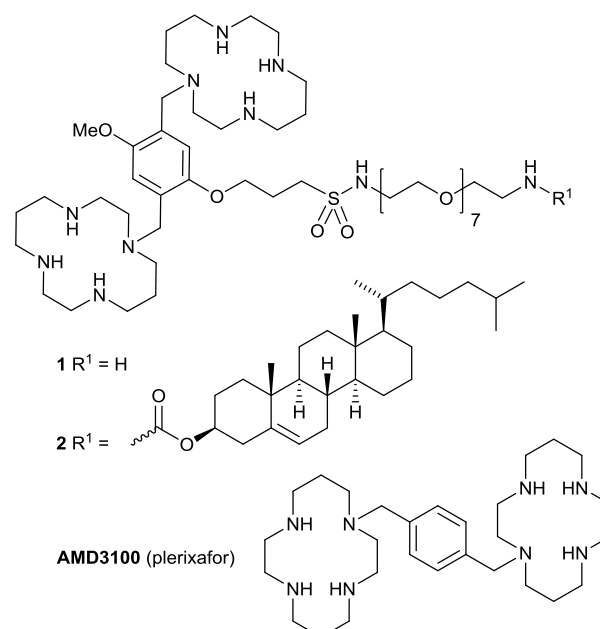


Figure 1. Bis(cyclam) conjugates 1, 2 and AMD3100.

Combination therapies that include AMD3100 have reached clinical trial in a range of cancers, both leukaemic and in solid tumours. It has been applied to enhance

^a School of Chemistry, University of Manchester, Oxford Road, Manchester M13 9PL, United Kingdom.

^b Manchester Institute of Biotechnology, University of Manchester, 131 Princess St, Manchester M1 7DN, United Kingdom. E-mail: S.Webb@manchester.ac.uk

^c Department of Haematology, Manchester Royal Infirmary, Manchester University NHS Foundation Trust, Manchester M13 9WL, United Kingdom

^d Division of Cancer Sciences, University of Manchester, Manchester, United Kingdom. E-mail: john.burthem@cmft.nhs.uk

^e Division of Pharmacy and Optometry, School of Health Sciences, University of Manchester, M13 9PL, United Kingdom.

† Contributed equally to the work.

Electronic Supplementary Information (ESI) available: Spectra for new compounds, VT NMR spectra, HPLC traces, DLS histograms, AFM images and Western Blots]. See DOI: 10.1039/x0xx00000x

immunotherapy and standard chemotherapeutics,^{11,12} underscoring the importance of the interaction between CXCR4 and cell chemotaxis, both with regards to metastasis and retention within chemoprotective niches.

The high affinity, small size, and well-established synthetic chemistry of the bis(cyclam) moiety make modification of this motif attractive, particularly for targeting cancer cells where the CXCR4 receptor is over-expressed. The high affinity of this class of molecule for CXCR4 ($K_i = 74$ nM for AMD3100)¹³ occurs because the bis(cyclam) motif binds tightly to two aspartate residues in CXCR4,¹⁴ specifically through interactions between the cyclams and the Asp171 and Asp262 residues, interactions that were uncovered through the introduction of point mutations in the receptor.^{13,15} It has been found that these interactions are strengthened if transition metal ions are complexed within the cyclam groups, with K_i values decreased approximately six-fold for zinc(II)-complexed AMD3100 when incubated with CXCR4-expressing COS-7 cells.¹⁶ Several groups have used bis(cyclam) motifs for targeted drug delivery to,^{17,18,19} or imaging of,^{19,20} cancer cells. Oupický *et al.* made bis(cyclam) polymers conjugated through the cyclams, and found the resulting nanoparticles were specifically taken up by cells overexpressing CXCR4. These polymers were used to deliver DNA as a therapeutic cargo; however, the affinity of the bis(cyclam) polymer for CXCR4 (measured in terms of antagonism against CXCR4 redistribution, $EC_{50} = 103$ ng/mL) was significantly lower than AMD3100 alone ($EC_{50} = 2$ ng/mL).^{17,18} A modified polymer with pendant and therefore less hindered cyclam groups was produced by the authors and found to have increased affinity ($EC_{50} = 21.3$ – 56.8 ng/mL, depending upon formulation) in comparison to previous polymeric forms.²¹ An analogue of AMD3100 for targeted imaging was created by Poty *et al.* using a seven step synthesis.^{20,22} This targeted PET radioligand had a ⁶⁸Ga complex appended to a bis(cyclam) core; the IC_{50} values for the compounds after attachment to the chelating group varied between 121–1485 nM, in comparison to 14 nM for AMD3100 (found in a competition assay against ¹²⁵I-CXCL12).²²

Although AMD3100 remains the only FDA-approved CXCR4-antagonist in clinical use, a variety of other CXCR4-antagonists have also been developed. AMD070 is another small molecule CXCR4 antagonist, which is of particular interest due to its oral bioavailability. It has reached Phase I/II clinical trials for use in the treatment of HIV, where its oral bioavailability is particularly desirable.²³ Cyclic pentapeptides have been extensively investigated since T140, a cyclic pentapeptide derived from horseshoe crab, was shown to have high affinity for CXCR4, albeit with low bioavailability. From structure-activity relationship studies on T140, a library of cyclic pentapeptide CXCR4 antagonists with high affinity to the receptor has since been developed, but bioavailability generally remains low.²³ Nevertheless, BL8040, a T140 analogue that is orally bioavailable, is an inverse agonist of CXCR4 that induces apoptosis of CXCR4-dependent cells *in vitro*. It has reached Phase II clinical trials for use alongside standard chemotherapeutics in acute myeloid leukaemia.^{23b,c}

In this work we present **2**, a lipid analogue of AMD3100 (Figure 1). This compound features a short octa(ethylene glycol) tether attached to the central aromatic ring, designed to provide flexibility to the bis(cyclam) binding group. At the end of this tether we have attached a lipid anchor, a cholesteryl group, which may lead to the self-assembly of **2** into nanoparticles that are taken up by cells or provide additional interactions with the membrane of the target cell. Several groups have found that adding a lipophilic region to a drug can improve targeting of the plasma membrane, leading to enhanced inhibition of HIV-1 infection, hepatitis B infection, BACE1 activity and GPCR signalling.²⁴ Similarly, it was hoped that cholesterol conjugation may reduce dimensionality and increase surface concentrations of **2**, improving its affinity for membrane receptors in comparison to non-lipidated counterparts.²⁵

The synthetic pathway towards **2** contains only four steps from commercially available advanced intermediates, or seven steps from commonly available reagents. This synthetic pathway will also provide amine-terminated bis(cyclam) **1**, which could be easily conjugated to fluorophores and nanoparticles for targeting of CXCR4-overexpressing cells.

Results and discussion

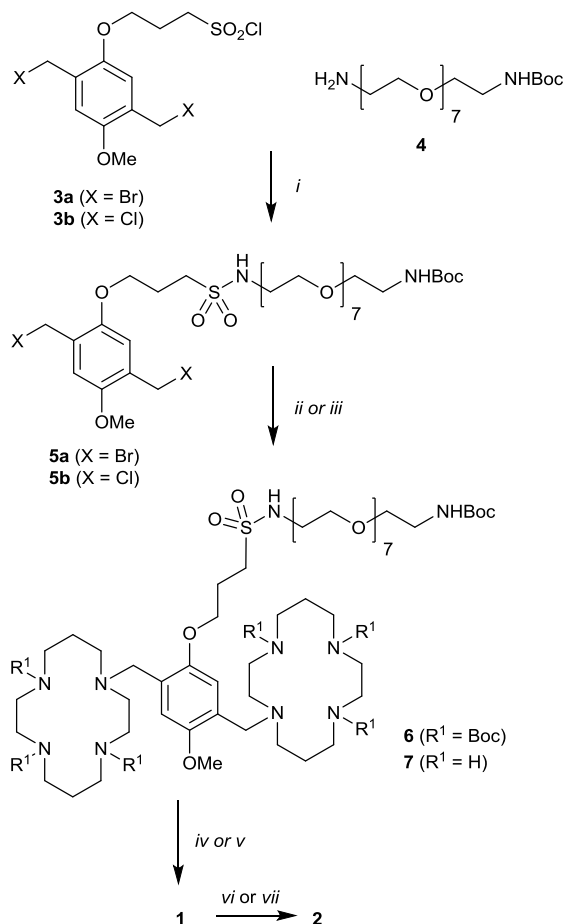
Synthesis of **1** and **2**

Compound **1** was designed to maintain both high affinity for CXCR4 and allow conjugation to biomolecules, drug delivery vehicles or imaging agents. Within the bis(cyclam) family of drugs, it is thought that the interaction with the CXCR4 receptor occurs predominantly through the cyclams, although changes to the spacer between the cyclam moieties can change overall geometry and conformation, and therefore alter affinity for the receptor.^{20,22,26} The structure of **1** includes an octa(ethylene glycol) (OEG) tether terminated with a primary amine, which is conjugated to the central aromatic region. This allows the bis(cyclam) moieties to be unimpeded while allowing simple conjugation to a wide range of different cargo.

The initial synthetic route was designed to provide key intermediate **1** in only three steps (Scheme 1), which we hoped would provide >100 mg of **1**, starting from commercially available sulfonyl chloride **3a**. The primary amine of **1** can then be easily conjugated to a lipid anchor. This synthetic approach was inspired by established methods for the synthesis of AMD3100, where triply protected cyclams are conjugated to the central aromatic region through bromomethyl “arms”.²⁷

Commercially available advanced intermediate **3a** was reacted with Boc protected OEG amine **4** to give crude sulfonamide **5a** in good yield (63 %). However analysis of the product showed multiplets at 4.62 and 4.52 ppm in the ¹H NMR spectrum and several peaks in the mass spectrum, both of which indicated partial displacement of the bromides by chloride during the reaction (the ¹H NMR spectrum shows *ca.* 50% exchange, with mass spectrometry showing peaks for the bis(chloride) (m/z 693), mixed chloride/bromide (m/z 739) and

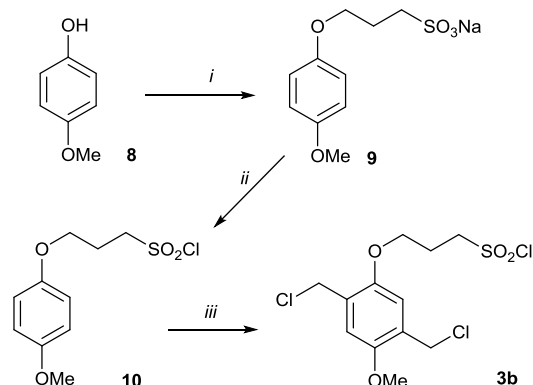
bis(bromide) (m/z 783) products, see the ESI). Treating the product mixture under Finkelstein conditions reinstated the bromides to give **5a**, but the intermediate compound with a mixture of chloride and bromides was found to be sufficiently reactive for the next synthetic step.



Scheme 1. Four step synthesis of **2**. i) 1.2 mol eq. DIPEA, 30 min sonication, 30 min stirring in dry DMF; ii) (Boc)₃cyclam (2.4 eq.), excess NaHCO₃, heated to reflux for 48 h in dry acetonitrile; iii) Cyclam (10 eq.), excess NaHCO₃, heated to reflux for 48 h in dry acetonitrile; iv) TFA, TFAA, CH₂Cl₂, RT, 4 h; v) 8 mol. eq. HCl in dry acetonitrile, 45 min; vi) Cholesteryl 3β-(*N*-hydroxysuccinimidyl)carbamate, excess NaHCO₃ in dry acetonitrile, 70 °C, overnight; vii) Cholesteryl 3β-(*N*-hydroxysuccinimidyl)carbamate, stir overnight in PBS (pH 7.4).

Literature precedent was followed to install two cyclams onto the central aromatic linker, using commercially available tri-Boc protected cyclam.²⁷ This step gave a moderate yield of the crude product, which required purification by HPLC. After purification on a C8 reverse phase column, using 0.1% (v/v) acetic acid in either water or acetonitrile as eluent, the protected bis(cyclam) **6** was obtained in 10 % yield. The solubility profile of the product **6** was poor, with low solubility in many common solvents. Furthermore, the resonances in the room temperature ¹H NMR spectrum of **6** in CD₃CN were all broad, as often observed for Boc substituted cyclams;²⁸ this made it difficult to assess the purity of the product from this step. However, VT NMR showed that increasing the

temperature sharpened all the resonances, and the ¹H NMR spectrum of **6** at 345 K in CD₃CN gave a sharp spectrum that permitted assignment of the resonances (see the ESI). Despite the successful purification of **6**, Boc deprotection of this compound using standard conditions (e.g. TFA and TFAA in CH₂Cl₂ at 0 °C), proved to be a challenging step. The removal of all seven protecting groups was relatively slow, with NMR spectroscopy showing that several Boc groups were still present even after 4 h at room temperature. The difficulty in removing all of the Boc groups was ascribed to the poor solubility of the partially deprotected intermediates. However, extending the reaction times and increasing the temperature led to significantly increased degradation of the product; analytical HPLC of the poorly soluble mixture showed several additional peaks were formed after 1 h and 2 h in the TFA mixture. Changing the deprotection conditions to HCl in acetonitrile led to successful deprotection and compound **1** could be obtained after HPLC purification (as the acetate salt due to acetic acid in the eluent) and characterised by ¹H NMR spectroscopy. However the yield for the key intermediate **1** was never higher than 10 % for these two steps from **5a**.



Scheme 2. Synthesis of 3-(2,5-bis(chloromethyl)-4-methoxyphenoxy)propane-1-sulfonyl chloride **3b**. i) 1,3-Propanesultone, NaOH, MeOH/1,4-dioxane; ii) SOCl₂, DMF; iii) Paraformaldehyde, CH₃CO₂H/HCl.

To improve the yield of **1**, two improvements in the synthesis were developed. Firstly although the advanced intermediate **3a** can be obtained commercially, this material is expensive and supply can be unreliable. We therefore decided to synthesise on a larger scale the corresponding chloride analogue **3b**, which is available in three simple steps (Scheme 2), then compare the reactivity of this bis(chloride) to that of the bis(bromide) **3a**. Secondly, an alternative subsequent route was devised, to give less protected intermediate compound **7** by using less expensive unprotected cyclam.

In the first of these modifications, 3-(2',5'-bis(chloromethyl)-4'-methoxyphenoxy)propane-1-sulfonyl chloride **3b** was obtained in an overall yield of 59 % in three simple and fast synthetic steps from 4-methoxyphenol **8**, following a modification of published procedures (Scheme 2).²⁹ Several key adjustments were discovered to be indispensable for this synthesis to be efficient. First, the activation of the propanesulfonate **9** to the propanesulfonyl chloride **10** has to be carried out using a concentrated suspension of **9**; even a

small 20 % increase in the amount of solvent caused a 30 % decrease in the yield of **10**. Furthermore using diethyl ether for the extraction of **10** turned out to be crucial to obtain a good yield. Compound **3b** initially precipitates out as a colloid, but reheating the suspension at 55 °C gives a thicker precipitate that can be easily filtered off. Reaction of **3b** with Boc-protected PEG amine **4** gave sulfonamide **5b** in good yield (75 %, Scheme 1). Intermediate **3b** was used without further transformation of the reactive arms from chloride to bromide as the chloromethyl groups were found to be sufficiently reactive in subsequent steps.

In the second modification, the reaction of sulfonamides **5a** or **5b** with unprotected cyclam to give **7** was proposed. This was hoped to be an economical alternative since only one Boc group must be removed from **7** to give **1**, allowing shorter deprotection times with concomitantly less degradation and fewer side-products. A ten-fold molar excess of cyclam was reacted with **5a** or **5b** under the same conditions employed to make **6**. After 48 h heating at reflux, the excess cyclam was filtered off, then the residue was purified using HPLC (reverse phase C8 column, mobile phase 0.1% (v/v) acetic acid in either water or acetonitrile) to afford the mono-Boc protected product **7** in a reasonable yield (e.g. 45 % from **5b**). This was a significant improvement in yield compared to the previous synthetic route and much of the excess cyclam could be recovered for future use. Unlike analogue **6** with seven Boc protecting groups, the ¹H NMR spectrum of **7** was as sharp at room temperature as that of **6** at elevated temperature (75 °C) and sharpens further as the temperature increase above room temperature (see the ESI), which indicates the role of multiple Boc groups in the slow conformational interconversion found for **6**. Compound **7** was then deprotected with hydrochloric acid in acetonitrile (8 eq. of acid, 37 % HCl in dry acetonitrile) at room temperature for 25 min. After purification on alumina the deprotected amine **1** was achieved in almost quantitative yield (90 %). The overall yield of **1** from 3-(2',5'-bis(chloromethyl)-4'-methoxyphenoxy)propane-1-sulfonyl chloride **3b** was 28 %, with 161 mg of key compound **1** obtained for further conjugation.

Following the successful synthesis of **1** in good yield, the acylation of the primary amine at the end of the OEG over the secondary amines in the cyclam groups was assessed. Initial investigations into the synthesis of the cholesterol conjugate showed that reaction with cholesterol chloroformate in DMF with DIPEA led to over-acylation, with up to three cholesterol units becoming conjugated to **1**, presumably by reaction with the secondary amines of the cyclam ring; MALDI mass spectrometry showed unreacted **1**, with additional peaks showing increases of 415 mass units. To overcome this problem, the reactivity of the acyl carbon was modulated by synthesising the corresponding *N*-hydroxysuccinimide (NHS) carbamate by reaction of the chloroformate with NHS in the presence of sodium hydrogen carbonate. Although **1** and the cholesteryl-NHS carbamate displayed rather different solubility profiles (**1** is most soluble in water), sonication was able to dissolve both reagents in acetonitrile to some extent. A slight excess of the amine **1** was used (1.2 eq.), as a dilute solution in

dry acetonitrile, and a solution of cholesteryl-NHS carbamate was added dropwise over 5 h. MALDI analysis of the fractions obtained after HPLC purification of the crude reaction mixture showed that the desired adduct had formed, mixed with both unreacted **1** and the adduct with two cholesterol units conjugated. Unfortunately, this method gave a yield <20 %, due in part to the insolubility of the reactants in a shared solvent and also by loss on the HPLC. To increase the solubility of both reagents, the reaction temperature was elevated to 70 °C. However the yield once again decreases, which might be due to degradation of the product at high temperatures. Finally, by reducing the cholesteryl-NHS addition time to 0.5 h, not sonicating, reacting overnight at 75 °C, and adding cholesteryl-NHS to the amine **1** in dry acetonitrile in a two to one ratio, the final product **2** was produced after HPLC purification in a yield of 36 %, which was a significant improvement to the previous procedures.

Self-assembly of **2** in aqueous media

Bis(cyclam) **2** was designed to be amphiphilic, with the lipophilic cholesterol region driving self-assembly into nanoparticles or enhancing interactions with the membrane of CLL cells. To assess the former, the self-assembly of **2** in water, both dynamic light scattering (DLS) and NMR spectroscopy were employed.

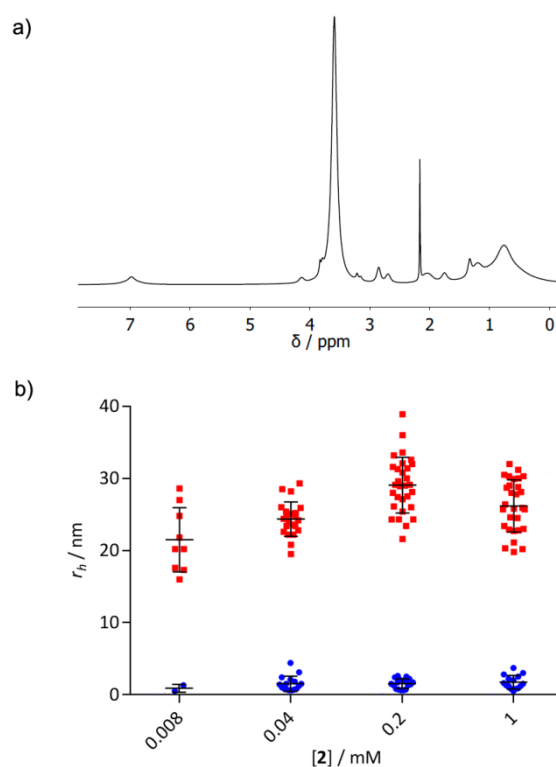


Figure 2. a) ¹H NMR spectrum of **2** in D₂O (13.9 mM), showing broad peaks due to self-assembly. Acetone added as a non-aggregating reference compound (sharp peak at 2.2 ppm). b) Dynamic light scattering (DLS) measurements of the hydrodynamic radii (r_h) of **2** dispersed in water. Each sample measured ten times and each preparation measured in triplicate. The hydrodynamic radius distribution was bimodal, with a population with r_h = 0 to 10 nm region (blue) and r_h = 10 to 40 nm (red). Each point indicates a mean radius measured on an individual run, while the black bars indicate the median and interquartile range across all measurements.

^1H NMR spectroscopy was first used to confirm the self-assembly of molecule **2** in aqueous media. Despite giving sharp peaks in the ^1H NMR spectrum when dissolved in CDCl_3 (see the ESI), when dispersed in D_2O significant signal broadening was observed in the spectrum (Figure 2 a). Such broadening is consistent with the presence of self-assembled particles or aggregates. An internal control, acetone, presented a sharp peak in the same spectrum.

Further to this outcome, the size of the self-assembled particles was investigated using DLS. Following the dispersal of molecule **2** in pure water by sonication, at concentrations from 2.56 nM to 1 mM, the hydrodynamic radii (r_h) of any particles in suspension were measured. These concentrations were selected as being within the range proposed for bioanalytical studies for targeting of CXCR4 on cells by **2** in suspension.

The presence of aggregates was observed at concentrations above 8 μM . This was the lowest concentration for which particles could be reliably observed and suggests that the critical aggregation concentration of **2** lies below this concentration. From 8 μM to 1 mM of **2**, the r_h distribution of the particles was found to be bimodal, with one population with radii between 0.9-1.7 nm, and another population with radii between 21.5-29.1 nm (Figure 2 b). Similar cholesteryl-PEG conjugates have been shown to form micelles. Chen *et al.* reported that micellar cholesterol-PEG2000-FITC had a hydrodynamic radius of 6.1 ± 1.2 nm,³⁰ while Yu *et al.* found that docetaxel-loaded cholesterol-PEG2000 micelles had an average hydrodynamic radius of 6.9 ± 0.3 nm.³¹ Micelles formed of **2** should be significantly smaller than those formed of PEG2000 given the 6-fold smaller chain length. The population of objects with r_h of 0.9-1.7 nm would therefore be consistent with micelles composed of **2**, with the population of larger objects perhaps due to further aggregation into vesicular, tape-like or sheet-like structures. Imaging of suspensions of **2** (100 μM) by atomic force microscopy (AFM) revealed a large number of self-assembled particles with radii typically in the range 6-40 nm, as well as some larger aggregates (e.g. 160 nm radius) (see the ESI). Both micelles and these larger structures would exhibit polyvalent displays of bis(cyclam) on the surface, which may enhance binding to cell surface CXCR4. The larger nanoscale objects may also be subject to endocytosis by targeted cells.³²

Biological activity of **2**

Receptor affinity (competition assay): Lipid **2** should interact with cells over-expressing CXCR4 through the bis(cyclam) motif binding to the receptor, but may have secondary interactions involving cholesterol and the cell membrane that may offer advantages over AMD3100. The self-assembly of the molecules in aqueous media could either increase or reduce the affinity of **2**, as polyvalent nanoparticles may either form multiple binding interactions or the bis(cyclam) may become hidden upon self-assembly. The binding affinity of **2** for CXCR4 expressed by primary CLL cells was therefore assessed using a competition assay with phycoerythrin-labelled CXCR4 antibody compared both to unconjugated **1** and to AMD3100 alone.

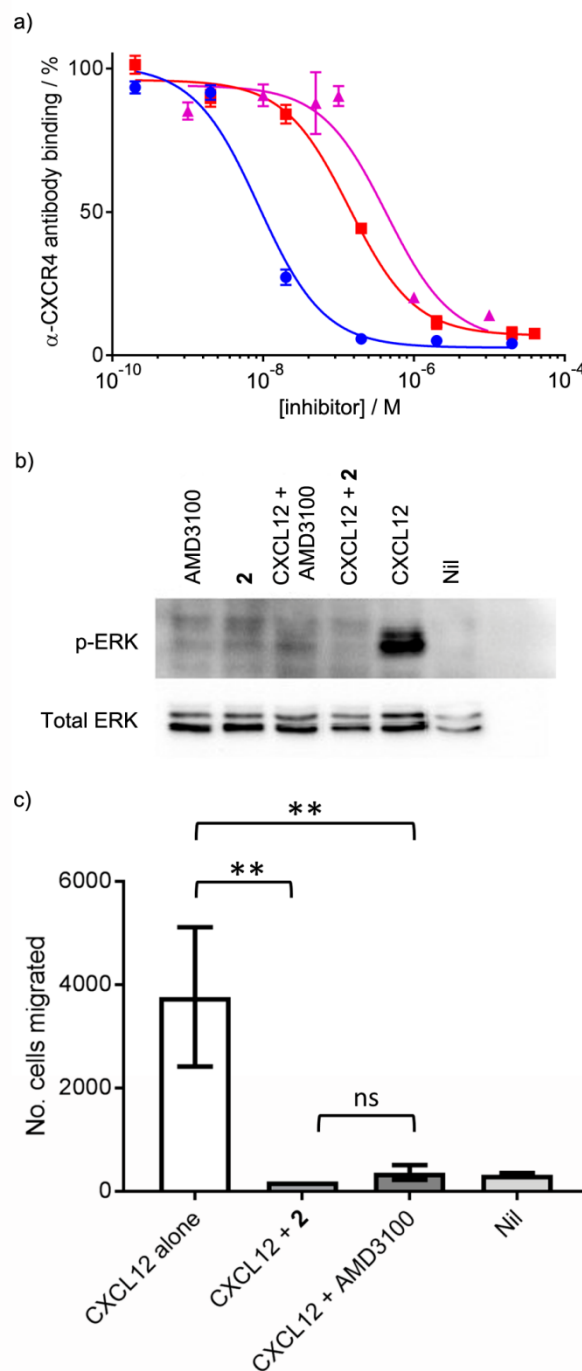


Figure 3. a) Competition assay of either AMD3100, **1**, or **2** against phycoerythrin-labelled CXCR4 antibody (PE- α -CXCR4) for CXCR4 on primary CLL cells; AMD3100 (\bullet , blue curve); **1** (\blacksquare , red curve); **2** (\blacktriangle , pink curve). Dose response curves assessed through flow cytometric analysis of a competition assay with PE- α -CXCR4, where both **1** and **2** show equivalent efficacy, but reduced potency compared to AMD3100. b) Western Blot of phosphorylated ERK (p-ERK) and total ERK. CXCL12 strongly induces phosphorylation of ERK compared with unstimulated control. This is blocked by **2** (20 μM) or AMD3100 (20 μM); neither drug alone induces signalling. c) Cell migration in response to CXCL12. CLL cell chemotaxis up a CXCL12 concentration gradient (200 ng/mL, after 1.5 h) through a filter migration (Transwell) assay. Pre-incubation (20 μM , 3 h) with **2** or AMD3100 reduced migration, comparable to nil stimulation. Statistical analysis performed using an ordinary one-way ANOVA, with Tukey's multiple comparisons test; $n = 3$. ns = not significantly different. ** $p \leq 0.01$.

A dose-dependent decrease in fluorescence with increasing concentration of either **1**, **2** or AMD3100 (used as a control) was observed (Figure 3a), which confirms specific binding of both **1** and **2** to CXCR4 receptors on the cell surface. The IC_{50} of **1** was found to be $0.139 \pm 0.003 \mu\text{M}$, whereas the IC_{50} of **2** was found to be $0.43 \pm 0.03 \mu\text{M}$; both are higher than AMD3100, where the IC_{50} was measured to be $8.8 \pm 0.7 \text{ nM}$ under these conditions. These data show that modification of the bis(cyclam) core causes the biggest drop in affinity (16-fold) compared to AMD3100, and addition of the cholesterol lipid anchor then further diminished the affinity of the key intermediate **1** for CXCR4 by *ca.* 4-fold. Although the interaction with CXCR4 takes place through the cyclams, alterations to the spacer region between the cyclams are also known to reduce the molecule's efficacy and potency.^{20,22,26} Nevertheless, both **1** and **2** retain good efficacy and this potency is comparable to other molecules of its class. Calculating the percentage antibody inhibition data under saturating conditions allows comparison with two non-metallated bis(cyclam) compounds reported by Poty *et al.*²⁰ Bis(cyclam) **1** showed ($93.2 \pm 1.4\%$) inhibition of antibody binding at $20 \mu\text{M}$ and **2** showed ($95.4 \pm 6.8\%$) at $10 \mu\text{M}$. Both values are higher than the reported inhibition values (*ca.* 45% at $20 \mu\text{M}$) for the non-metallated bis(cyclams) (substituted on the aryl spacer), which were measured against a 12G-5 PE-conjugated antibody.²⁰

Effect on CXCL12-induced downstream signalling: After confirming that **2** specifically binds CXCR4 in an antibody competition assay, its antagonistic effect was confirmed. The signalling cascade following CXCR4/CXCL12 complexation involves the RAS/RAF/MEK/ERK pathway, where ERK phosphorylation leads to chemotaxis, transcription and gene expression.³³ A Western Blot was performed to assess ERK phosphorylation following incubation with CXCL12, carried out in the presence or absence of either **2** or AMD3100. The blot confirmed that CXCL12 strongly induces ERK phosphorylation in the CLL lymphocytes. Neither **2** nor AMD3100 demonstrated any agonist effect, but each prevented the CXCL12-induced ERK phosphorylation (Figure 3b). In a control assay, stimulation of the B-cell receptor also strongly induced ERK phosphorylation, but this was not inhibited by **2** or by AMD3100, confirming that the inhibitory effects of **2** and AMD3100 are specific to CXCR4-CXCL12 interactions (see the ESI).

Effect on chemotaxis along CXCL12 gradients: In addition to pro-survival signalling, the ligand CXCL12 is known to play a significant role in the emigration into and retention of CLL cells within protective niches such as the bone marrow and lymphoid organs. Production of CXCL12 by cells that are present in these environments (such as macrophages and mesenchymal stromal cells) causes CLL cells to move along the concentration gradient and into the tissues. To confirm that **2** could effectively disrupt CLL cell migration into and residence within these protective niches, it is important to observe that **2**

inhibits CXCL12-induced cell chemotaxis in culture. The chemotaxis of cells up a CXCL12 concentration gradient was assessed using a filter migration (Transwell) assay; aliquots of cell suspensions that had been treated with **2**, AMD3100 or PBS respectively were transferred into the upper chamber of a Transwell plate and the lower chamber was filled with CXCL12 in media. After 90 mins incubation, the number of cells present in the lower chamber was counted using flow cytometry, to give a measure of the cells' ability to move directionally through a barrier in response to CXCL12 following CXCR4 blockade (Figure 3c).

In the presence of CXCL12 alone, high levels of migration through the Transwell membrane were observed. However pre-incubation with **2** ($20 \mu\text{M}$, 3 h) strongly reduced cell migration, and was comparable to AMD3100 inhibition or nil stimulation. These results suggest that **2** disrupts the CXCR4/CXCL12 signalling pathway, which leads to reduced chemotaxis. This activity could therefore reduce cells' migration into chemoprotective niches in CLL, as well as metastasis in other implicated cancers.

Conclusions

We have developed a rapid seven step synthesis to give a cholesterol functionalised bis(cyclam), with an overall yield of 17% from 4-methoxyphenol **8** (or *ca.* 30% from the commercially available advanced intermediate **3a**). This pathway provided access to >50 mg of the target compound, as well as the important bis(cyclam) intermediate **1** that has a primary amine for functionalisation. Conditions were developed that allowed the unprotected bis(cyclam) **1** to be selectively modified on this primary amine.

The cholesterol tail on bis(cyclam) lipid **2** was hoped to interact with the membranes of targeted cells, combining this hydrophobic interaction with binding of the bis(cyclam) to the cell surface CXCR4 receptor, and/or to drive self-assembly of **2** into nanoparticles that can be taken up by cells. Although the hydrophobic tail led to self-assembly in water, giving both micelles and non-micellar structures around 30 nm in diameter, adding the cholesterol tail to **1** to give **2** did not improve affinity for CXCR4 in primary CLL cells. Although sub-micromolar affinities of **2** for CXCR4 were measured ($0.4 \mu\text{M}$), this was 4-fold weaker than the affinity of **1** for CXCR4 and 50-fold weaker than the affinity of the archetypical bis(cyclam) drug AMD3100 for CXCR4. Despite this lower affinity for CXCR4, bioconjugate **2** was as effective as AMD3100 (both at $20 \mu\text{M}$) in reducing chemotaxis along CXCL12 gradients, showing that **2** may be effective in disrupting migration of CLL cells into protective niches, such as the bone marrow and lymphoid organs. This disruption has been observed for AMD3100 during *in vivo* experiments and in clinical practice,¹⁻⁵ but further work *in vivo* would be needed to confirm this effect for **2**. In future, transition metal ion complexation to **1** and **2** could be employed to boost affinities for CXCR4; metalation has been shown to significantly increase the affinities of other bis(cyclam) drugs for CXCR4.

Although use of **2** alone provided no advantage over AMD3100, the lipid anchor on **2** provides several new applications. It will allow decoration of liposomes with bis(cyclam) motifs, where the cholesterol anchor mediates insertion of **2** into the membrane of drug-loaded liposomes. Such bis(cyclam) coated liposomes would have dual functionality, delivering the liposomal cargo to cancer cells over-expressing CXCR4 while retaining the anti-migration properties of **2**. Such bis(cyclam)-coated liposomes would have the potential for the addition of further targeting functionality, such as glycolipids,³⁴ and/or a triggered release mechanism.³⁵ It should also be noted that Linning *et al.* found that the tether length between their BACE1-inhibiting molecule and the lipid anchor was fundamental in the activity of their molecule;^{24c} therefore, future work may include the alteration of the length of the OEG tether in **2**. Key intermediate **1** should also find many other applications as the primary amine permits bioimaging groups, such as fluorophores, MRI contrast agents or PET imaging agents, to be ligated to the CXCR4-targeting bis(cyclam). Further investigations into biomedical applications of both **1** and **2** are ongoing.

Experimental

Materials and methods

3-[2',5'-Bis(chloromethyl)-4-methoxyphenoxy]-1-propanesulfonyl chloride, *N,N*-di-*iso*-propylethylamine (99.5% biotech. grade with Sure/SealTM), 1,4,8,11-tetraazacyclotetradecane (98%), 2,2,2-trifluoroacetic acid and trifluoroacetic anhydride, cholesteryl chloroformate and all deuterated solvents were obtained from Sigma-Aldrich® Co. (UK). *N,N*-Dimethylformamide (99.8% extra dry with AcroSeal), acetonitrile (99.9%, extra dry with AcroSeal), chloroform, petroleum ether, dichloromethane, acetonitrile, methanol, diethyl ether and ethyl acetate (all Analytical Reagent Grade) were obtained from Fisher Scientific. *O*-(2-Aminoethyl)-*O'*-[2-(Boc-amino)ethyl]hexaethylene glycol was obtained from Polypure AS, Norway.

Nuclear Magnetic Resonance (NMR) spectra were recorded on a Bruker Ultrashield 400 or 500 MHz spectrometer in CDCl₃, D₂O or CD₃OD. ¹H and ¹³C spectra were referenced relative to the solvent residual peaks and chemical shifts (δ) reported in ppm downfield of tetramethylsilane. Coupling constants (*J*) are reported in Hertz and rounded to 0.1 Hz. Splitting patterns are abbreviated as follows: singlet (s), doublet (d), triplet (t), quintet (quin), multiplet (m), broad (br) or a combination of these.

Mass spectra were recorded by staff at the University of Manchester. High resolution mass spectra (HRMS) were recorded on a Thermo Finnigan MAT95XP mass spectrometer and analysed using the in-built Agilent MassHunter Workstation software; all HRMS values are accurate to ± 0.001 Da. Thin layer chromatography (TLC) was performed using commercially available pre-coated plates (Macherey Nagel alugram. Sil G/UV254); phosphomolybdic acid dip and UV light were used to visualise the products. Flash

column chromatography was carried out using Sigma-Aldrich silica 40-63 μ m particle size, 60 Å pore size.

Semi-preparative high pressure liquid chromatography (HPLC) purification was performed on HPLC Agilent 1100 series equipped with a semi-preparative C8 column Agilent eclipse XDB-C8, 5 μ m, 9.4 mm \times 250 mm. Analytical HPLC was performed using the Agilent 1260 Infinity LC with an Agilent ZORBAX Eclipse XDB reverse phase C8 column (150 \times 4.6 mm) with a 5 μ m particle size. Preparative HPLC was on a DuPont Instruments Zorbax C8 column, (21.2 mm \times 25 cm) with 5 μ m particle size.

Flow cytometry was performed using a BD FACSCanto™ II flow cytometer with two lasers (488 nm solid state and 633 nm HeNe) and analysed using BD FACSDiva™ and Flowing Software v 2.5.

Synthetic procedures

Sodium 3-(4'-methoxyphenoxy)propane-1-sulfonate 9: Method adapted from the literature,²⁹ ¹³C NMR data reported here for the first time. 4-Methoxyphenol **8** (4.00 g, 32.22 mmol) was dissolved in MeOH/Dioxane (1:1 vol/vol, 100 mL). NaOH powder (1.30 g, 32.5 mmol) was added in portions. After the NaOH was fully dissolved, 1,2-oxathiolane 2,2-dioxide (3.94 g, 32.2 mmol) was added. The reaction mixture was stirred overnight, and the resulting white precipitate was filtered and dried under vacuum, giving **9** as a white powder (7.31 g, 27.3 mmol, 85%). ¹H NMR (400 MHz, D₂O, 298 K) δ ppm 2.04 - 2.15 (quin, *J* = 7.7 Hz, 2 H), 2.99 (t, *J* = 7.7 Hz, 2 H), 3.72 (s, 3 H), 4.05 (t, *J* = 6.2 Hz, 2 H), 6.86 - 6.95 (m, 4 H); ¹³C NMR (100 MHz, D₂O, 298 K) δ ppm 24.2, 47.8, 55.9, 67.6, 115.1, 116.4, 152.3, 153.4; HRMS (ESI): *m/z* calcd. for C₁₀H₁₃Na₁O₅S + K⁺: 307.0002, found: 307.0013.

3-(4'-Methoxyphenoxy)propane-1-sulfonyl chloride 10: Using a method adapted from the literature.²⁹ Sodium 3-(4'-methoxyphenoxy)propane-1-sulfonate **9** (1.00 g, 3.73 mmol) were suspended in dry DMF (3 mL). Thionyl chloride (1.5 mL, 20.65 mmol) was added dropwise at 0 °C and the resulting yellow suspension was allowed to stir at room temperature for 2 h. Afterwards the reaction mixture was added to ice water (50 mL) to quench the excess thionyl chloride (caution: toxic vapours). The aqueous layer was extracted with diethyl ether (2 \times 20 mL). The organic layer was washed with cold water (20 mL) and dried over MgSO₄. Filtration and evaporation of the solvent afforded (0.93 g, 3.52 mmol, 94 %) of a pale yellow liquid, which becomes a yellow solid after cooling to 4 °C. The sulfonyl chloride **10** was used without further purification.

3-(2',5'-bis(chloromethyl)-4'-methoxyphenoxy)propane-1-sulfonyl chloride 3b: Method adapted from the literature,²⁹ ¹³C NMR data reported here for the first time. 4-Methoxyphenol **8** (4.00 g, 32.22 mmol) was dissolved in MeOH To a stirred suspension of 3-(4'-methoxyphenoxy)propane-1-sulfonyl chloride, **10** (0.5 g, 1.9 mmol) and paraformaldehyde (0.153 g, 5.1 mmol) in glacial acetic acid (3 mL) was added dropwise a mixture of concentrated hydrochloric acid (1 mL) in glacial acetic acid (2.5 mL) at room temperature. Then the reaction mixture was stirred at 85 °C for 4 h resulting in a clear

yellow liquid. After the clear liquid cooled to room temperature, it was poured into water (10 mL) and a fine white solid was formed. The suspension was heated at 55 °C for another 10-15 min to form a thick precipitate. The white solid was collected by filtration and dried under vacuum for 24 h (0.51 g, 1.4 mmol, 74 %). ¹H NMR (400 MHz, CDCl₃, 298 K) δ ppm 2.53 - 2.62 (m, 2 H), 3.87 (s, 3 H), 3.98 (t, *J* = 8.5 Hz, 2 H), 4.21 (t, *J* = 5.7 Hz, 2 H), 4.63 (s, 2H), 4.65 (s, 2 H), 6.91 (s, 1 H), 6.94 (s, 1 H); ¹³C NMR (100 MHz, CDCl₃, 298 K) δ ppm 24.9, 41.0, 41.5, 56.3, 62.4, 65.6, 113.5, 114.5, 127.1, 127.3, 149.8, 151.6; HRMS (ESI): *m/z* calcd for C₁₂H₁₅Cl₃O₄S - H⁺: 358.9687, found: 358.9684

tert-Butyl (23-((3-(5-(bromomethyl)-2-(chloromethyl)-4-methoxyphenoxy)propyl)sulfonamido)-3,6,9,12,15,18,21-heptaaxatricosyl)carbamate 5a:

3-(2,5-Bis(bromomethyl)-4-methoxyphenoxy)-1-propanesulfonyl chloride (450 mg, 1.03 mmols) **3a**, *O*-(2-aminoethyl)-*O'*-[2-(Boc-amino)ethyl]hexaethylene glycol **4** (390 mg, 0.86 mmols), *N,N*-di-*iso*-propylethylamine (DIPEA) (143 μL, 1.03 mmols) were added to dry CHCl₃ under inert conditions and the reaction was sonicated for 30 mins and then stirred for a further 30 mins. The CHCl₃ and DIPEA were then removed under reduced pressure using a rotary evaporator. The crude mixture was re-dissolved in chloroform and purified using flash column chromatography (10% (v/v) methanol in chloroform on silica), giving **5a** as a yellow oil (476 mg, 0.54 mmol, 63%). *R_f*: 0.78 (10% (v/v) methanol in chloroform on silica, silica pre-flushed with 100% chloroform). For analytical purposes, the chloro-substituted arms were exchanged for bromines under Finkelstein conditions: to a solution of **5a** (35 mg, 42 μmols) in dry dimethylformamide (DMF) (5 mL) was added an excess of sodium bromide (26 mg, 252 μmols); the mixture was kept stirring overnight. The DMF was then removed under reduced pressure and the mixture redissolved in in CDCl₃. Excess sodium salts were removed via filtration for analysis. ¹H NMR (400 MHz, CDCl₃, 298 K) δ ppm 1.37 (s, 9 H), 2.29 (m, 2H), 3.26 (m, 6 H), 3.47 (t, *J* = 5 Hz, 2 H), 3.52-3.60 (m, 26 H), 3.80 (s, 3 H), 4.07 (t, *J* = 5.74 Hz, 2H), 4.42 (s, 2 H), 4.45 (s, 2 H), 5.06 (br s, 1 H), 5.59 (br s, 1 H), 6.78 (s, 1 H), 6.80 (s, 1 H); ¹³C NMR (125 MHz, CDCl₃, 298 K) δ ppm 24.1, 28.4, 28.8, 40.36, 43.1, 49.6, 56.2, 66.6, 70.06, 70.1, 70.3, 70.4, 79.2, 113.7, 114.7, 127.4, 127.6, 150.2, 151.5, 156.1 HRMS (ESI): *m/z* calcd for C₃₃H₅₈Br₂N₂O₁₃S + Na⁺: 903.1919, found: 903.1919.

tert-Butyl (23-((3-(2,5-bis((1',4',8'-tri(*tert*-butoxycarbonyl)-1',4',8',11'-tetraazacyclotetradecan-11'-yl)methyl)-4-methoxyphenoxy)propyl)sulfonamido)-3,6,9,12,15,18,21-heptaaxatricosyl)carbamate 6:

Molecule **5a** (50 mg, 56 μmol) and tri-*tert*-butyl 1,4,8,11-tetraazacyclotetradecane-1,4,8-tricarboxylate (67 mg, 134.4 μmol) were added to dry acetonitrile with sodium carbonate (12 mg, 112 μmol) and left stirring for 48 h under reflux. The reaction mixture was filtered using fluted filter paper to remove the sodium carbonate and the solvent was removed under reduced pressure using a rotary evaporator. The crude mixture was directly purified using HPLC on a C8 reverse phase column using two solvent systems, solvent A (0.1% (v/v) acetic acid in water) and solvent B (0.1% (v/v) acetic acid in acetonitrile), in

the gradient - A (%): 80-60 (0-5 mins), 60-50 (5-40 mins), 50-0 (40-50 mins), 0 (50-60 mins). This provided **6** (9 mg, 5.5 μmol, yield 9.8 %). ¹H NMR spectra were recorded at 293 K and 345 K, with the increase in temperature providing sharper resonances.²⁴ ¹H NMR (400 MHz, CD₃CN, 293 K) δ ppm 1.27 - 1.49 (m, 64 H), 1.70 (br s, 4 H), 1.85 (br s, 4 H), 2.15 - 2.25 (m, 4 H), 2.41 (br s, 4 H), 2.54 - 2.65 (m, 3 H), 2.95 - 3.42 (m, 31 H), 3.47 (t, *J* = 5.6 Hz, 3 H), 3.52 (br s, 2 H), 3.53 - 3.61 (m, 28 H), 3.76 (s, 3 H), 4.04 (br t, *J* = 5.9 Hz, 2 H), 5.29 - 5.53 (m, 1 H), 5.54 - 5.76 (m, 1 H), 6.87 (br s, 1 H), 6.93 (br s, 1 H). ¹H NMR (500 MHz, CD₃CN, 345 K) δ ppm 1.28 (d, *J* = 1.9 Hz, 17 H), 1.31 - 1.32 (m, 1 H), 1.32 (s, 17 H), 1.33 (s, 9 H), 1.35 (s, 19 H), 1.59 (br s, 5 H), 1.79 (br dd, *J* = 14.0, 7.1 Hz, 6 H), 1.73 - 1.81 (m, 1 H), 2.07 - 2.15 (m, 2 H), 2.33 (br d, *J* = 6.0 Hz, 4 H), 2.53 (dt, *J* = 14.9, 5.6 Hz, 4 H), 3.09 (q, *J* = 5.9 Hz, 2 H), 3.12 - 3.16 (m, 4 H), 3.16 - 3.28 (m, 25 H), 3.38 (t, *J* = 5.5 Hz, 2 H), 3.44 (s, 2 H), 3.45 - 3.48 (m, 23 H), 3.49 (s, 4 H), 3.67 (s, 3 H), 3.95 (t, *J* = 6.1 Hz, 2 H), 5.10 (br s, 1 H), 5.29 (br s, 1 H), 6.79 (s, 1 H), 6.84 (s, 1 H); HRMS (ESI): *m/z* calcd. for C₈₃H₁₅₂N₁₀O₂₅S + H⁺: 1722.0729, found: 1722.0668.

tert-Butyl (23-((3-(2,5-bis(chloromethyl)-4-methoxyphenoxy)propyl)sulfonamido)-3,6,9,12,15,18,21-heptaaxatricosyl)carbamate 5b:

3-[2,5-Bis(chloromethyl)-4-methoxyphenoxy]-1-propanesulfonyl chloride (371 mg, 1.03 mmols) **3b**, *O*-(2-aminoethyl)-*O'*-[2-(Boc-amino)ethyl]hexaethylene glycol **4** (390 mg, 0.86 mmols), *N,N*-diisopropylethylamine (DIPEA) (143 μL, 1.03 mmols) were added to dry CHCl₃ under inert conditions and the reaction was sonicated for 30 mins and then stirred for a further 30 mins. The CHCl₃ and DIPEA were then removed under reduced pressure using a rotary evaporator. The crude mixture was re-dissolved in chloroform and purified using flash column chromatography (10% (v/v) methanol in chloroform on silica), giving **5b** as a yellow oil (610 mg, 0.77 mmol, 75%). *R_f*: 0.79 (10% (v/v) methanol in chloroform on silica, silica pre-flushed with 100% chloroform). ¹H NMR (400 MHz, CDCl₃, 298 K) δ ppm 1.43 (s, 9 H) 2.30-2.37 (m, 2 H) 3.26 - 3.34 (m, 6 H) 3.52 (t, *J* = 5.1 Hz 2 H) 3.59 - 3.64 (m, 26 H) 3.85 (br s, 3 H) 4.11 - 4.14 (m, 2 H) 4.60 (s, 2 H), 4.61 (s, 2 H) 5.09 (br s, 1 H), 5.44 (br s, 1 H), 6.89 (br s, 1 H) 6.92 (br s, 1 H); ¹³C NMR (400 MHz, CDCl₃, 298 K) δ ppm 24.0, 28.4, 29.7, 40.4, 41.2, 41.5, 42.8, 43.1, 49.2, 49.5, 56.3, 66.9, 69.8, 69.8, 70.0, 70.0, 70.1, 70.1, 70.1, 70.2, 70.2, 70.4, 70.5, 70.5, 113.4, 114.5, 126.9, 127.3 150.2, 151.4, 156.0; HRMS (ESI): *m/z* calcd for C₃₃H₅₇Cl₂N₂O₁₃S⁻: 791.2978, found: 791.2964.

tert-Butyl (23-((3-(2,5-bis((1',4',8',11'-tetraazacyclotetradecan-11'-yl)methyl)-4-methoxyphenoxy)propyl)sulfonamido)-3,6,9,12,15,18,21-heptaaxatricosyl)carbamate 7:

Molecule **5b** (569 mg, 0.648 mmol) and 1,4,8,11-tetraazacyclotetradecane (cyclam, 779 mg, 3.89 mmol) were added to dry acetonitrile (30 mL) with sodium hydrogen carbonate (436 mg, 5.18 mmol) and left stirring for 48 h under reflux. The reaction mixture was filtered using fluted filter paper to remove the sodium hydrogen carbonate and excess unreacted cyclam, and the solvent was removed under reduced pressure using a rotary evaporator. The crude mixture was purified using reverse phase C8

preparative HPLC with a mobile phase composed of water and acetonitrile with 0.1% (v/v) acetic acid in the gradient – A (%): 80-60 (0-5 mins), 60-50 (5-40 mins), 50-0 (40-50 mins), 0 (50-60 mins) to afford a yellow oil (327 mg, 0.292 mmol, 45%). R_f : 11.46 mins. $^1\text{H NMR}$ (500 MHz, CD_3OD , 348 K) δ ppm 1.34 (s, 9 H), 1.70-1.78 (m, 4 H), 1.86-1.97 (m, 4 H), 2.18 (quin, $J = 6.6$ Hz, 2 H), 2.56-2.66 (m, 8 H), 2.74-2.84 (m, 8 H), 2.90-2.96 (m, 4 H), 2.95-3.06 (m, 12 H), 3.11 (t, $J = 5.7$ Hz, 2 H), 3.16 (t, $J = 5.2$ Hz, 2 H), 3.18-3.20 (m, 2 H), 3.40 (t, $J = 5.5$ Hz, 2 H), 3.45-3.59 (m, 26 H), 3.69 (s, 2 H), 3.78 (s, 5 H), 4.09 (t, $J = 6.1$ Hz, 2 H), 6.87 (s, 2 H); $^{13}\text{C NMR}$ (100 MHz, D_2O , 298 K) δ ppm 21.9, 22.1, 22.9, 24.6, 27.7, 39.6, 42.1, 44.1, 44.3, 44.7, 44.8, 46.4, 46.5, 46.7, 46.8, 48.2, 48.5, 49.2, 50.5, 50.70, 50.8, 52.1, 53.7, 57.1, 67.09, 69.4, 69.45, 69.5, 80.9, 117.3, 118.2, 123.6, 124.1, 151.0, 152.3, 158.2; HRMS (ESI): m/z calcd for $\text{C}_{53}\text{H}_{104}\text{N}_{10}\text{O}_{13}\text{S} + 2\text{H}^+$: 561.3825, found: 561.3836.

23-((3-(2,5-bis((1',4',8',11'-tetraazacyclotetradecan-11'-yl)methyl)-4-methoxyphenoxy)propyl)sulfonamido)-

3,6,9,12,15,18,21-heptaaxatricosylamine 1: Concentrated hydrochloric acid (37 %, 8 eq.) was added to **7** (0.175 mmol, 196 mg) dissolved in dry acetonitrile and the mixture was stirred under an inert atmosphere at room temperature for 25 minutes. The acetonitrile and HCl were removed under reduced pressure and the residue was kept under vacuum for a further 24 h to remove any residual solvent or acid. Crude white solid was purified on neutral aluminium oxide (activated, neutral, Brockmann 1, 150 Mesh) (90% (v/v) acetonitrile in Water); R_f : 0.36. This afforded **1** as a waxy transparent solid that became pale yellow upon dissolution in solvents (161 mg, 0.157 mmol, 90 %). $^1\text{H NMR}$ (500 MHz, D_2O , 298 K) δ ppm 1.80 – 1.69 (m, 4H), 2.03 (s, 4H), 2.18 (quin, $J = 6.4$ Hz, 2H), 2.75 – 2.61 (m, 8H), 2.88 – 2.78 (m, 8H), 3.24 – 2.98 (m, 22H), 3.29 (t, $J = 7.6$ Hz, 2H), 3.55 (t, $J = 5.2$ Hz, 2H), 3.65 – 3.57 (m, 24H), 3.68 (t, $J = 4.8$ Hz, 2H), 3.80 (s, 3H), 3.84 (s, 2H), 4.15 (t, $J = 6.3$ Hz, 2H), 6.94 (s, 1H), 6.96 (s, 1H); $^{13}\text{C NMR}$ (125 MHz, D_2O , 298 K) δ ppm 22.9, 23.2, 23.2, 23.3, 24.7, 24.7, 39.3, 42.1, 44.9, 45.1, 45.2, 45.3, 45.3, 46.1, 46.8, 47.0, 47.1, 48.5, 49.1, 49.2, 49.4, 49.6, 49.7, 51.0, 51.2, 53.2, 54.0, 57.1, 57.1, 58.8, 67.3, 68.3, 68.3, 68.4, 69.4, 69.5, 69.6, 69.6, 69.6, 116.5, 118.1, 124.9, 125.7, 150.8, 152.4. HRMS (ESI): m/z calcd for $\text{C}_{48}\text{H}_{96}\text{N}_{10}\text{O}_{11}\text{S} + \text{H}^+$: 1021.70535, found: 1021.7019

Cholester-3''-yl (23-((3-(2,5-bis((1',4',8',11'-tetraazacyclotetradecan-11'-yl)methyl)-4-methoxyphenoxy)propyl)sulfonamido)-3,6,9,12,15,18,21-

heptaaxatricosyl)carbamate 2: Cholesteryl chloroformate (1.00 g, 2.23 mmol), NHS (307 mg, 2.67 mmol) and triethylamine (74 μL , 5.34 mmol) were dissolved in CH_2Cl_2 (200 mL) and stirred overnight at 0 °C. The reaction mixture was washed with 1 M HCl and brine. The organic layer was dried over MgSO_4 and filtered. The solvent was removed from the filtrate under reduced pressure (0.82 g, 83 %) to obtain the cholesteryl-NHS carbamate as a white solid, which was used without further purification. To a suspension of molecule **1** (64 mg, 0.063 mmol) and NaHCO_3 (42 mg, 0.50 mmol) in dry acetonitrile (60 mL) was added the cholesteryl-NHS carbamate (68 mg, 0.126 mmol) in dry acetonitrile (25 mL) dropwise over 0.5 h. The resulting suspension was stirred at 75 °C overnight.

The acetonitrile was removed under reduced pressure. The crude product was washed with diethyl ether (20 mL) to remove unreacted cholesteryl-NHS carbamate. The compound was then dissolved in chloroform (60 mL) and the remaining NaHCO_3 and **1** were removed through filtration, affording a pale, yellow oil, which was purified using reverse phase C8 preparative HPLC with a mobile phase composed of water (A) and acetonitrile (B) with 0.1% (v/v) acetic acid in the gradient – A (%): 95-80 (0-5 mins), 80-50 (5-10 mins), 50-0 (10-50 mins), 0 (50-70 mins), 0-95 (70-80 mins). The final product was a pale yellow oil (66 mg, 0.046 mmol, 73%). $^1\text{H NMR}$ (400 MHz, CDCl_3 , 298 K) δ ppm 0.61 (s, 3H), 0.79 (dd, $J = 6.6, 1.9$ Hz, 6H), 0.84 (d, $J = 6.5$ Hz, 3H), 0.87 – 0.97 (m, 5H), 0.98 – 1.34 (m, 6H), 1.34 – 1.54 (m, 6H), 1.71 – 1.84 (m, 6H), 1.85 – 1.98 (m, 6H), 2.17 – 2.25 (m, 2H), 2.25 – 2.33 (m, 2H), 2.53 – 2.64 (m, 8H), 2.78 – 2.86 (m, 8H), 2.86 – 2.94 (m, 8H), 2.94 – 3.01 (m, 4H), 3.18 (br t, $J = 7.5$ Hz, 2H), 3.23 (t, $J = 5.5$ Hz, 2H), 3.29 (dt, $J = 5.1, 5.2$ Hz, 2H), 3.45 – 3.51 (m, 4H), 3.51 – 3.61 (m, 24H), 3.69 (s, 3H), 3.70 (s, 2H), 3.84 (s, 2H), 4.01 (t, $J = 5.9$ Hz, 2H), 4.37 – 4.47 (m, 1H), 5.18 (t, 2H), 5.27 – 5.32 (m, 1H), 6.68 (s, 1H), 6.75 (s, 1H); $^{13}\text{C NMR}$ (126 MHz, CDCl_3) δ ppm³⁶ 11.9, 18.7, 19.4, 21.0, 22.6, 22.8, 23.8, 23.9, 24.3, 24.6, 25.9, 27.8, 28.0, 28.2, 28.2, 28.4, 29.7, 31.9, 31.9, 35.8, 36.2, 36.6, 37.0, 38.6, 39.5, 39.7, 40.7, 42.3, 42.8, 45.9, 46.0, 46.1, 47.8, 48.2, 48.5, 49.0, 49.1, 49.2, 49.7, 49.8, 50.0, 50.7, 53.1, 53.4, 56.1, 56.3, 56.7, 61.8, 66.9, 70.1, 70.3, 70.3, 70.3, 70.4, 70.5, 70.5, 70.6, 70.6, 70.6, 70.7, 70.7, 72.5, 74.3, 115.3, 116.5, 122.5, 124.1, 125.0, 139.9, 151.1, 152.3, 156.2; HRMS (ESI): m/z calcd for $\text{C}_{76}\text{H}_{140}\text{N}_{10}\text{O}_{13}\text{S} + \text{K}^+$: 1471.9954, found: 1471.9998.

Self-assembly assays

NMR spectroscopy of **2** in D_2O : $^1\text{H NMR}$ spectroscopy was performed using a 400 MHz spectrometer at 298 K, with **2** at a concentration of 13.9 mM in D_2O . Dynamic light scattering (DLS): Aggregate sizes of **2** were assessed in MilliQ® water at concentrations between 2.56 nM-1 mM using a Wyatt DynaPro Plate Reader, with a 633 nm laser and a scattering angle of 173°. Ten scans were completed for each sample, where each scan was 5 s and each sample was prepared in triplicate. All measurements were performed at 25 °C. Atomic Force Microscopy (AFM): Suspensions of **2** in MilliQ® water were drop-cast onto freshly cleaved mica for 120 s, after which any excess moisture was wicked away and the surface washed with MilliQ® water. The substrates were allowed to dry overnight. The surfaces were imaged using a Bruker Multimode in ScanAsyst® mode, and Nanoscope® and Gwyddion 2.51 were used for image analysis. The AFM tip was a ScanAsyst-Air, with tip radius 2 nm.

Biological assays

Cell culture: Primary CLL lymphocytes were cultured in RPMI 1640 (Sigma Aldrich, UK) supplemented with 10% foetal calf serum (FCS), 1% L-glutamine, 1% penicillin streptomycin (ThermoFisher, UK). Primary CLL lymphocytes were taken from liquid nitrogen storage; these had been collected from CLL patients with full Research Ethics Committee (REC) approval for use in evaluation of new treatment strategies (REC reference 10/H1017/73). All samples had been collected with

full consent for research use and are stored in pseudo-anonymised form with identity traced only through the collecting medical institution (Manchester Royal Infirmary, custodian Dr John Burthem). There are no direct or indirect medical implications for donors. AMD3100, **1** and **2** were used without pre-complexation to zinc(II) or other metal ions. It should be noted, however, that cells were cultured in media with 10 % FCS; FCS contains *ca.* 40 μM zinc (II),³⁷ so adventitious complexation of some zinc(II) may occur *in situ*.

Flow cytometry: The antibody competition assay was developed by modification of a published procedure.³⁸ Primary CLL cells were cultured for 24 h at 2×10^6 cells/mL in a 96-well plate (300 μL) before incubation with antagonist in the concentration range 0.2 nM – 20 μM for 3 h or PBS (-ve control). An aliquot of each sample (100 μL) was harvested and stained with fluorescent labelled anti-CXCR4 antibody (10 μL of the supplied solution of mouse anti-human PE-conjugated monoclonal CXCR4 antibody (clone #44717), R&D Systems®, UK) on ice for 30 mins, then fixed with paraformaldehyde in PBS (final conc. 1 %). Samples were diluted with PBS (300 μL) then analysed by flow cytometry (BD FACS Canto™ II, analysis performed using BD FACSDiva™ and Flowing Software v 2.5) with 10000 events recorded for each sample, and all were illuminated using a laser of $\lambda_{\text{ex}} = 633$ nm. The IC_{50} values for **1**, **2** and AMD3100 were determined using non-linear regression with a 3 parameter Hill equation (GraphPad Prism v 7.03).

Western Blot: Primary CLL cells were cultured overnight in a 24 well plate with 6×10^6 cells/well. Cells were then exposed to **2** or AMD3100 at 20 μM , or PBS for 3 h before incubating with CXCL12 at 200 ng/mL for 10 mins at 37 °C, before placing on ice. A control blot where the B-cell receptor was activated was also performed: cells were exposed to biotinylated anti-IgM followed by avidin to cross-link the receptor in the presence or absence of **2** or AMD3100 (see the ESI). Cells were lysed and cytosolic proteins extracted with RIPA buffer (50 mM Tris, 150 mM NaCl, 1 % (v/v) Triton-X-100, 0.25 % (w/v) sodium deoxycholate, 1 mM EDTA, pH 7.4). The extracted protein in Laemmli buffer with 5 % β -mercaptoethanol was loaded onto a 10 % SDS-PAGE gel then blotted onto a PVDF membrane (Amersham™ Hybond® P Western Blotting membranes, Sigma Aldrich, UK). The membranes were incubated with phospho-p44/42 MAPK (Erk1/2) rabbit monoclonal antibody (#9102 Cell Signaling Technology®) at 1:1000 overnight at 4 °C, following which they were exposed to the secondary antibody (NA934V, ECL™ anti-rabbit IgG HRP-linked whole antibody, GE Healthcare Life Sciences) at 1:10000 for an hour at room temperature. Visualisation of bound antibody employed Amersham ECL Prime Western Blotting Detection Reagent using a Bio-Rad™ Chemidoc XRS Molecular Imager and Image Lab™ software. A loading-control blot was performed for total ERK using p44/42 MAPK (Erk1/2) (9102, Cell Signaling Technology®).

Transwell assays: Primary CLL cells were cultured overnight at a density of 1×10^7 cells/mL, before incubation with **2** or AMD3100 at 20 μM , or plain PBS for 3 h. The cells were then aliquoted into the inserts of a Transwell plate (Sarstedt, UK)

and the well underneath was filled with 600 μL complete media with or without CXCL12 (carrier-free, R&D Systems, UK) at 200 ng/mL; the cells were incubated for a further 90 mins at 37 °C. The bottom well was then agitated and 400 μL of the media removed for cell counting. Samples were passed through a flow cytometer at a consistent flow rate for 30 s to give a cell number relative to the positive control (CXCL12 with no antagonist).

Conflicts of interest

There are no conflicts to declare.

Acknowledgements

This work was supported by a University of Manchester EPSRC Doctoral Prize Award, an EPSRC NOWNANO DTC studentship (grant number EP/G03737X/1), funding from the Manchester Pharmacy School (University of Manchester, UK) and a Colloid Science PhD studentship from the School of Chemistry (University of Manchester, UK). We thank Mrs. Rehana Sung for her guidance in developing HPLC protocols and the School of Chemistry's nuclear magnetic resonance (NMR) spectroscopy service. We also thank Dr. Reynard Spiess and the Mass Spectrometry Service in the School of Chemistry (University of Manchester) for mass spectrometry support. Finally, we thank Dr. Nigel Hodson (BioAFM Facility, University of Manchester) for his help in both preparing the samples and performing AFM imaging.

Abbreviations

BACE1, β -site APP cleaving enzyme 1; BM, bone marrow; Boc, *tert*-butyloxycarbonyl; CLL, chronic lymphocytic leukaemia; CXCR4, C-X-C chemokine receptor type 4; CXCL12, C-X-C motif chemokine ligand 12; DLS, dynamic light scattering; DMF, *N,N*-dimethylformamide; EC_{50} , half maximal effective concentration; ESI, electrospray ionisation; FCS, foetal calf serum; HIV, human immunodeficiency virus; HPLC, high performance liquid chromatography; IC_{50} , half maximal inhibitory concentration; MALDI, matrix assisted laser desorption/ionization; NHS, *N*-hydroxysuccinimide; OEG, octa(ethylene glycol); PBS, phosphate buffered saline; PE, R-phycoerythrin; TFA, trifluoroacetic acid; TFAA, trifluoroacetic anhydride; TLC, thin layer chromatography.

References

- 1 E. De Clercq, *Biochem. Pharmacol.*, 2009, **77**, 1655–1664.
- 2 U. M. Domanska, R. C. Kruijzinga, W. B. Nagengast, H. Timmer-Bosscha, G. Huls, E. G. E. de Vries and A. M. E. Walenkamp, *Eur. J. Cancer*, 2013, **49**, 219–230.
- 3 B. Stamatopoulos, N. Meuleman, C. De Bruyn, K. Pieters, P. Mineur, C. Le Roy, S. Saint-Georges, N. Varin-Blank, F. Cymbalista, D. Bron and L. Lagneaux, *Haematol. Hematol. J.*, 2012, **97**, 608–615.
- 4 J. A. Burger and A. Peled, *Leukemia*, 2009, **23**, 43–52.

- 5 J. A. Burger, P. Ghia, A. Rosenwald, and F. Caligaris-Cappio, *Blood*, 2009, **114**, 3367-3375.
- 6 L. Reinholdt, M. B. Laursen, A. Schmitz, J. S. Bødker, L. H. Jakobsen, M. Bøgsted, H. E. Johnsen and K. Dybkær *Biomark. Res.*, 2016, **4**, 12.
- 7 D. Heckmann, P. Maier, S. Laufs, F. Wenz, W. J. Zeller, S. Fruehauf and H. Allgayer, *Transl. Oncol.*, 2013, **6**, 124-132.
- 8 U. M. Domanska, H. Timmer-Bosscha, W. B. Nagengast, T. H. O. Munnink, R. C. Kruizinga, H. J. K. Ananias, N. M. Kliphuis, G. Huls, E. G. E. De Vries, I. J. de Jong and A. M. E. Walenkamp, *Neoplasia*, 2012, **14**, 709-718.
- 9 A. K. Azab, J. M. Runnels, C. Pitsillides, A.-S. Moreau, F. Azab, X. Leleu, X. Jia, R. Wright, B. Ospina, A. L. Carlson, C. Alt, N. Burwick, A. M. Roccaro, H. T. Ngo, M. Farag, M. R. Melhem, A. Sacco, N. C. Munshi, T. Hideshima, B. J. Rollins, K. C. Anderson, A. L. Kung, C. P. Lin and I. M. Ghobrial, *Blood*, 2009, **113**, 4341-4351.
- 10 T. T. Price, M. L. Burness, A. Sivan, M. J. Warner, R. Cheng, C. H. Lee, L. Olivere, K. Comatas, J. Magnani, H. K. Lyerly, Q. Cheng, C. M. McCall and D. A. Sipkins, *Sci. Transl. Med.*, 2016, **8**, 340ra73.
- 11 (a) Y. Chen and D. G. Duda, *Oncolmmunology*, 2015, **4**, e1029703; (b) C. Feig, J. O. Jones, M. Kraman, R. J. B. Wells, A. Deonaraine, D. S. Chan, C. M. Connell, E. W. Roberts, Q. Zhao, O. L. Caballero, S. A. Teichmann, T. Janowitz, D. I. Jodrell, D. A. Tuveson and D. T. Fearon, *Proc. Natl. Acad. Sci. U.S.A.* 2013, **110**, 20212-20217; (c) L. Andritsos, J. C. Byrd, J. A. Jones, B. Hewes, T. J. Kipps, F. J. Hsu and J. A. Burger, *Blood*, 2010, **116**, 2450; (d) L. Andritsos, J. Byrd, B. Hewes, T. Kipps, D. Johns and J. Burger, *Haematologica*, 2010, **95** (Suppl. 2), Abstract 0772.
- 12 D. M. Brander, S. D. Allgood, D. A. Rizzieri, T. Stewart, J. B. Weinberg and M. C. Lanasa, *Blood*, 2014, **124**, 5658.
- 13 L. O. Gerlach, R. T. Skerlj, G. J. Bridger and T. W. Schwartz, *J. Biol. Chem.*, 2001, **276**, 14153-14160.
- 14 X. Liang and P. J. Sadler, *Chem. Soc. Rev.*, 2004, **33**, 246-266.
- 15 S. Hatse, K. Princen, L.-O. Gerlach, G. Bridger, G. Henson, E. De Clercq, T. W. Schwartz and D. Schols, *Mol. Pharmacol.*, 2001, **60**, 164-173.
- 16 L. O. Gerlach, J. S. Jakobsen, K. P. Jensen, M. R. Rosenkilde, R. T. Skerlj, U. Ryde, G. J. Bridger and T. W. Schwartz, *Biochemistry*, 2003, **42**, 710-717.
- 17 (a) J. Li, Y. Zhu, S. T. Hazeldine, C. Li and D. Oupický, *Angew. Chem. Int. Ed.*, 2012, **51**, 8740-8743; (b) J. Li and D. Oupický, *Biomaterials*, 2014, **35**, 5572-5579.
- 18 Y. Wang, J. Li and D. Oupický, *Pharm. Res.*, 2014, **31**, 3538-3548.
- 19 Y. Wang, J. Li, Y. Chen and D. Oupický, *Biomater. Sci.*, 2015, **3**, 1114-1123.
- 20 S. Poty, P. Désogère, C. Goze, F. Boschetti, T. D'huys, D. Schols, C. Cawthorne, S. J. Archibald, H. R. Maëcke and F. Denat, *Dalton Trans.*, 2015, **44**, 5004-5016.
- 21 Y. Wang, S. T. Hazeldine, J. Li and D. Oupický, *Adv. Healthcare Mater.* 2015, **4**, 729-738.
- 22 S. Poty, E. Gourni, P. Désogère, F. Boschetti, C. Goze, H. R. Maecke and F. Denat, *Bioconjug. Chem.*, 2016, **27**, 752-761.
- 23 (a) B. Debnath, S. Xu, F. Grande, A. Garofalo and N. Neamati, *Theranostics*, 2013, **3**, 47-75; (b) G. Borthakur, A. Nagler, Y. Ofran, J. M. Rowe, J. K. Altman, O. Frankfurt, M. S. Tallman, I. Avivi, A. Peled, Y. Pereg, A. Foley-Comer, L. Russovsky, A. Aharon, T. McQueen, N. Pemmaraju, C. E. Bueso-Ramos, J. E. Cortes and M. Andreeff, *Blood*, 2014, **124**, 950; (c) M. Abraham, S. Klein, B. Bulvik, H. Wald, I. D. Weiss, D. Olam, L. Weiss, K. Beider, O. Eizenberg, O. Wald, E. Galun, A. Avigdor, O. Benjamini, A. Nagler, Y. Pereg, S. Tavor and A. Peled, *Leukemia*, 2017, **31**, 2336-2346.
- 24 (a) P. Ingallinella, E. Bianchi, N. A. Ladwa, Y.-J. Wang, R. Hrin, M. Veneziano, F. Bonelli, T. J. Ketas, J. P. Moore, M. D. Miller, and A. Pessi, *Proc. Natl. Acad. U.S.A.*, 2009, **106**, 5801-5806; (b) J. Petersen, M. Dandri, W. Mier, M. Lütgehetmann, T. Volz, F. von Weizsäcker, U. Haberkorn, L. Fischer, J.-M. Pollok, B. Erbes, S. Seitz and S. Urban, *Nat. Biotechnol.* 2008, **26**, 335-341; (c) P. Linning, U. Hausmann, I. Beyer, S. Weidlich, H. Schieb, J. Wiltfang, H.-W. Klafki and H.-J. Knölker, *Org. Biomol. Chem.*, 2012, **10**, 8216-8235; (d) L. Covic, M. Misra, J. Badar, C. Singh and A. Kuliopulos, *Nat. Med.* 2002, **8**, 1161-1165; (e) L. Covic, A. L. Gresser, J. Talavera, S. Swift and A. Kuliopulos, *Proc. Natl. Acad. U.S.A.*, 2002, **99**, 643-648.
- 25 L. Rajendran, H.-J. Knölker and K. Simons, *Nat. Rev. Drug Discov.*, 2010, **9**, 29-42.
- 26 (a) G. J. Bridger, R. T. Skerlj, D. Thornton, S. Padmanabhan, S. A. Martellucci, G. W. Henson, M. J. Abrams, N. Yamamoto, K. De Vreese, R. Pauwels and E. De Clercq, *J. Med. Chem.*, 1995, **38**, 366-378; (b) Y. Inouye, T. Kanamori, M. Sugiyama, T. Yoshida, T. Koike, M. Shionoya, K. Enomoto, K. Suehiro and E. Kimura, *Antivir. Chem. Chemother.*, 1995, **6**, 337-344.
- 27 (a) S. Brandes, C. Gros, F. Denat, P. Pullumbi and R. Guillard, *Bull. Soc. Chim. Fr.* 1996, **133**, 65-73; (b) D. Guillaume and G. R. Marshall, *Synth. Commun.*, 1998, **28**, 2903-2906.
- 28 (a) M. Yu, G. Nagalingam, S. Ellis, E. Martinez, V. Sintchenko, M. Spain, P. J. Rutledge, M. H. Todd and J. A. Triccas, *J. Med. Chem.*, 2016, **59**, 5917-5921; (b) Y. H. Lau, J. K. Clegg, J. R. Price, R. B. Macquart, M. H. Todd, P. J. Rutledge, *Chem. Eur. J.* 2018, **24**, 1573-1585.
- 29 (a) S. Shi and F. Wudl, *Macromolecules*, 1990, **23**, 2119-2124; (b) Y. Zhang, M. Xin, W. Lin, Z. Yu, J. Peng, K. Xu, M. Chen, *Synth. Met.* 2014, **193**, 8-16.
- 30 X. Chen, X. Zhang, H.-Y. Wang, Z. Chen and F.-G. Wu, *Langmuir*, 2016, **32**, 10126-10135.
- 31 Y. Yu, Y. He, B. Xu, Z. He, Y. Zhang, Y. Chen, Y. Yang, Y. Xie, Y. Zheng, G. He, J. He and X. Song, *J. Pharm. Sci.*, 2013, **102**, 1054-1062.
- 32 S. Behzadi, V. Serpooshan, W. Tao, M. A. Hamaly, M. Y. Alkawareek, E. C. Dreaden, D. Brown, A. M. Alkilany, O. C. Farkhad and M. Mahmoudi, *Chem. Soc. Rev.*, 2017, **46**, 4218-4244.
- 33 B. A. Teicher and S. P. Fricker, *Clin. Cancer Res.* 2010, **16**, 2927-2931.
- 34 (a) G. T. Noble, F. L. Craven, J. Voglmeir, R. Šardžik, S. L. Flitsch and S. J. Webb, *J. Am. Chem. Soc.* 2012, **134**, 13010-13017; (b) F. L. Craven, J. Silva, M. D. Segarra-Maset, K. Huang, P. Both, J. E. Gough, S. L. Flitsch and S. J. Webb, *Chem. Commun.*, 2018, **54**, 1347-1350.
- 35 (a) F. de Cogan, A. Booth, J. E. Gough and S. J. Webb, *Angew. Chem. Int. Ed.*, 2011, **50**, 12290-12293; (b) A. Booth, I. C. Pintre, Y. Lin, J. E. Gough and S. J. Webb, *Phys. Chem. Chem. Phys.*, 2015, **17**, 15579-15588.
- 36 The ¹³C NMR peaks at 125.0 and 124.1 ppm were identified in the HMBC spectrum. See the ESI.
- 37 Y.-E. Cho, R.-A. R. Lomeda, S.-H. Ryu, J.-H. Lee, J. H. Beattie and I.-S. Kwun, *Nutr. Res. Pract.* 2007, **1**, 29-35.
- 38 T. Murakami, S. Kumakura, T. Yamazaki, R. Tanaka, M. Hamatake, K. Okuma, W. Huang, J. Toma, J. Komano, M. Yanaka, Y. Tanaka and N. Yamamoto, *Antimicrob. Agents Chemother.*, 2009, **53**, 2940-2948.